

Dissipative Particle Dynamics Study of Order–Order Phase Transition of BCC, HPC, OBDD, and LAM Structures of the Poly(styrene)–Poly(isoprene) Diblock Copolymer

César Soto-Figueroa,[†] María-del-Rosario Rodríguez-Hidalgo,^{*,†}
José-Manuel Martínez-Magadán,[‡] and Luis Vicente[§]

Departamento de Ciencias Químicas, Facultad de Estudios Superiores Cuautitlán, Universidad Nacional Autónoma de México Av. 1° de Mayo s/n Campo 1. Cuautitlán Izcallí, 54740. Estado de México, México; Programa de Ingeniería Molecular, Instituto Mexicano del Petróleo, Eje Central Lázaro Cárdenas 152, 07730 México, D.F. México, and Departamento de Física y Química Teórica, Facultad de Química, Universidad Nacional Autónoma de México, 04510 México, D.F. México

Received December 19, 2007; Revised Manuscript Received February 27, 2008

ABSTRACT: A Gaussian chain model of poly(styrene)–poly(isoprene) (PS–PI) block copolymer with a dissipative particle dynamics (DPD) simulation was employed to study the formation of specific characteristic structures such as body-centered-cubic (BCC), hexagonal packed cylinders (HPC), ordered bicontinuous double diamond (OBDD), and lamellar (LAM) via order–disorder transition (ODT). The BCC, HPC, OBDD and LAM microphases were then subjected to thermal cycles of heating and cooling. The order–order phase transition (OOT) from HPC to BCC was monitored and two new transitions, OBDD to LAM and LAM to hexagonal perforated layers (HPL), were detected during the thermal process. Two metastable states (cylinders and HPL) were observed in the OOT process from the OBDD to LAM microphases. It is shown that all order–order transitions between the different kinds of structures are thermoreversible. The results were compared with the predictions of recent theories and with available experimental outcomes and thus provide a test for the predictions of BCC, OBDD, and LAM microphases.

I. Introduction

Block copolymers form a particularly interesting kind of amphiphilic material composed of sequences, or blocks, of chemically distinct repeat units. In the melted phase, these polymeric materials can self-assemble into a variety of ordered structures via the process of microphase separation. The microphase segregation in these materials is driven by enthalpic and entropic thermodynamic interactions that govern the demixing process of the constituent components. The enthalpic contributions in the microphase separation process are proportional to the Flory–Huggins segmental interaction parameter χ that describes the repulsive interaction between different components due to chemical incompatibility between the polymers. That is, the magnitude of χ is determined by selection of the A–B monomer pair and has a temperature dependency. χ is found to be inversely proportional to temperature and is usually parametrized as $\chi \approx dT^{-1} + \beta$.^{1,2} The entropic interactions in the microphase separation process describe the configurational and translational chain displacement and are regulated by the overall degree of polymerization N , architecture constraints, and composition.

The mean-field theory (MFT) of Leibler³ predicts that the behavior of and microphase separation in asymmetric diblock copolymers depends on the enthalpic–entropic balance and can be expressed by the reduced parameter χN . When the value of this parameter attains a critical value, $(\chi N)_{\text{ODT}} = 10.5$, stable ordered structures evolve out of the system in the disordered state. This phase transition is termed the order–disorder phase transition (ODT). Depending on the degree of incompatibility χN , several segregation regimens (weak segregation limit

(WSL), intermediate, and strong segregation limit (SSL)) have been reported.⁴ In the weak segregation limit, the block copolymers are characterized by a widened interface due to enhanced phase mixing. In the vicinity of this regime, thermotropic phase transitions between different kinds of microdomain structures of block copolymers can be predicted. Fredrickson and Helfand⁵ have extended Leibler's result for fluctuation effects, following a procedure developed by Brazovskii.⁶ This led to the prediction of the phase transition between different structures, where the transition from one ordered state is referred to as the order–order transition (OOT).^{7,8} The induced thermal behavior from the characteristic ordered state of block copolymers is thus an interesting topic with respect to microphase modification.

Recent studies have been reported on the order–order phase transition of poly(styrene)–poly(isoprene) diblock copolymers. They are determined experimentally by either rheology^{9–12} or small-angle X-ray (or neutron) scattering (SAXS or SANS)^{13–16} methods. Most of these studies account for the order–order transition from cylindrical microdomains to a spheres arrangement of pure block copolymers and its binary mixtures. Sakurai et al.¹⁷ experimentally confirmed the existence of an OOT between cylinders and spheres of poly(styrene)–poly(isoprene) diblock copolymer, and they observed the thermoreversible morphology transition. This fact agrees with Leibler's weak segregation limit theory and specifically with the schematic representation of the phase diagram of upper critical solution temperature, as shown in Figure 1. According to this figure, it is possible to predict equilibrium morphology changes and multiple ordered states from temperature effects in other structures different from the hexagonal packed cylinders. Modi,¹⁸ Kim,¹⁹ and Ryu²⁰ have proposed possible ordering kinetics of the order–order phase transition from hexagonal cylinders to a spheres arrangement in a diblock copolymer. Furthermore, this order–order transition is thermally reversible, although the kinetics of the spheres-to-cylinder transition is

* Corresponding author.

[†] Departamento de Ciencias Químicas, Facultad de Estudios Superiores Cuautitlán, Universidad Nacional Autónoma de México.

[‡] Programa de Ingeniería Molecular, Instituto Mexicano del Petróleo.

[§] Departamento de Física y Química Teórica, Facultad de Química, Universidad Nacional Autónoma de México.

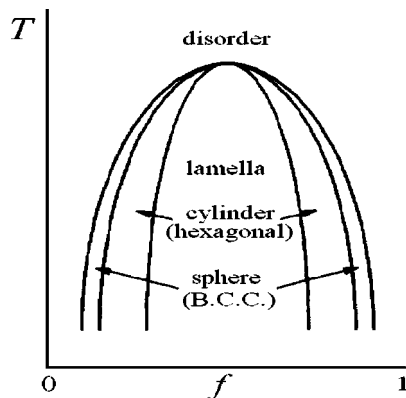


Figure 1. Phase diagram of temperature vs composition (volume fraction) version of that proposed by Leibler³ for diblock copolymers in the weak segregation limit. In this schematic representation, it is possible to see equilibrium morphology changing from the lamellar to the disordered state via cylinders and spheres.

considerably slower than that of the cylinder-to-spheres transition. On the other hand, Kimishima et al.²¹ indicate that the cylinder-to-spheres and spheres-to-cylinder thermoreversible transitions are likely rather straightforward: the cylinder breaks up into spheres. This process is induced by the thermodynamic instability between the microdomain interfaces. Though the order–order transition has been reported in the cylinder-to-spheres system, the thermal transition process of other ordered microphases such as LAM, BCC, and OBDD have not been reported yet in detail. The methods employed to characterize the OOT process, such as TEM, SAXS, and SANS, required freezing the sample during the OOT process. This fact generates disarray in the memory of in situ processes, and therefore, the metastable states during order–order transition cannot be observed in detail. The order–order transition phenomenon that is generated in thermal processes can be explored in more detail through mesoscopic dynamic simulations than in an experiment.

It is well-known that the PS–PI diblock copolymer can generate a variety of well defined ordered microphases. A property of this copolymer is its ability to self-organize in the melted phase or in solution into a variety of ordered structures with characteristic dimensions in the range of a few nanometers up to several micrometers. This polymeric material affords a unique opportunity for a detailed study of thermodynamics processes such as microphase transitions and self-assembly processes (order–order and order–disorder). The self-organization process in a PS–PI diblock copolymer is controlled by the microphase separation thermodynamics that arise from the

repulsive interaction of its chemically dissimilar components (chemical incompatibility between styrene and isoprene chains) and is driven by the enthalpy and entropy of demixing of the constituent components of the block copolymer. The enthalpic–entropic balance governing the structural self-organization via a microphase separation process in these materials can be controlled by the composition of the copolymer. This fact has been exploited in previous works.^{22–24}

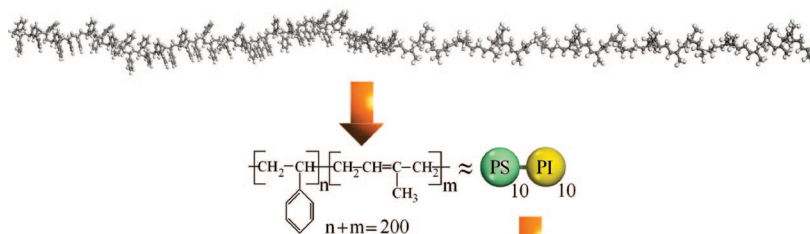
In this work, we explored the microphase evolution process of equilibrium ordered structures with defined PS–PI diblock copolymer morphologies from a mesoscopic point of view by dissipative particle dynamics simulations. The thermotropic order–order phase transition process and the multiple ordered states were analyzed for each ordered microphase (BCC, HPC, OBDD and LAM).

This paper is organized as follows. In section 2, we briefly present the Gaussian chain model parametrization and mesoscale simulation method applied to study the PS–PI phase behavior. Section 3 contains our main results and a discussion of order–disorder and order–order phase transition processes monitored from the mesoscopic simulation. This section is divided into two parts. In the first part, we present detailed results of the microphase separation process. The ordered structure formation via the order–disorder transition process was analyzed by changing the composition of the copolymers. In the second part, we discuss our findings regarding the microphase evolution process as a function of temperature (order–order transition process) from the ordered structures obtained in the first part of the section. In section 4, our conclusions are presented.

2. Model and Mesoscale Simulation Method

2.1. Gaussian Chain Model Parametrization of the PS–PI Copolymer. The molecular structure of the poly(styrene)–poly(isoprene) diblock copolymer, designated as PS–PI, was built via the Polymer Builder Module.²⁵ The polymeric molecule contains a total of 200 repetitive units in the diblock chain, and its linear architecture is characteristic of this system (Figure 2a). The molecular weight of the PS–PI copolymer is in the range 13985–20466. The PS–PI molecular structure was subject to a study of conformational properties via RIS Metropolis Monte Carlo simulations. All single and partial double bonds in the block chain were allowed to rotate during the molecular simulation except those involving bonds of the rings of the polystyrene fragment. The PPS–PI system was described by the Gaussian chain model,²⁶ which was constituted of beads connected through harmonic springs, where each spherical bead represented a segment with a statistical distribution of the PS–PI copolymer. In previous papers,^{22,23} we

a) PS–PI copolymer structure



b) Gaussian chain model of PS–PI system

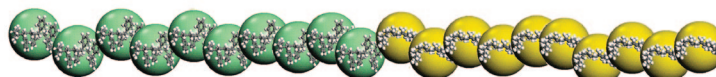


Figure 2. Schematic representation of the bead-spring chain model of the poly(styrene)–poly(isoprene) diblock copolymer: (a) PS–PI diblock copolymer structure with linear architecture; (b) Gaussian chain model (mechanical model of PS–PI system).

have shown that the characteristic ratio (statistical distribution) gives reliable results in order to describe the poly(styrene)–poly(isoprene) system. Therefore, we have employed this statistical segment level for mapping the molecular structure of linear diblock copolymers into Gaussian chain models. The number of beads in each statistical model was determined using the molar mass of each block copolymer, molar mass of a repeat unit, degree of polymerization, and $\langle C_n \rangle$ the characteristic ratio of each polymeric system. A more detailed description of the conformational properties and the mapping of atomistic structures to a mesoscale model is given in Soto-Figueroa et al.²⁴ In this way the PS–PI copolymer is represented by a mechanical model constituted of 20 spherical beads denoted by $[\text{PS}]_n - [\text{PI}]_m$, as sketched schematically in Figure 2b. In this figure, the mechanical model is constructed with identical lines of $(\text{PS}_n - \text{PI}_m)$ diblock fragments, and the linear diblock copolymer is described by one linear chain. The Gaussian chain model developed for the PS–PI copolymer describes the real molecular structure at the characteristic ratio statistical segment level where the atomistic details are ignored.

As in previous works,^{23,24} the quantitative estimate of the bead–bead interaction for a mechanical model has been calculated from the monomer–monomer interaction using the Flory–Huggins thermodynamic model.^{27,28} In this theory, the key parameter is the so-called Flory–Huggins interaction parameter $\chi(T)$, which can be evaluated by means of molecular simulations using the Fan et al.²⁹ model. In this extension of the Flory–Huggins model, the molecules are not arranged on a planar lattice as in the original Flory–Huggins theory, but they are arranged off-lattice (three-dimensional).

The interaction parameter between different segments in the Gaussian model is given by the magnitude of repulsion between different repetitive units. The fundamental parameters, which include the heat of mixing associated with styrene–isoprene molecular interactions and the numbers of possible interaction partners, i.e., coordination number, $Z_{12}(T)$, and interaction energies, $\Delta E_{12}(T)$, were obtained by averaging a large number of generated configurations (typically 500000). The bead–bead interaction between different segments is given by the magnitude of repulsion between different repetitive units. For example, at a temperature of 300 K, the styrene–isoprene (monomer–monomer) molecular interaction parameter obtained from a simulation is $\chi = 0.3955$. Since the average number of repetitive units of PS and PI beads is 10 units per bead for both polymers, then the bead–bead interaction parameter is $\chi = 3.955$. Molecular interaction parameters obtained from Monte Carlo simulations are comparable with those achieved from experimental data (solubility parameters)³⁰ using the Flory–Huggins relation.³¹ More details regarding the temperature dependence of interaction parameters in the range 200–500 K, solubility parameters and experimental data are given in Soto-Figueroa et al.²⁴ It is important to keep in mind that a reliable and realistic value of $\chi(T)$ is necessary since it is used as an input in the DPD simulation. All beads in the mechanical model are assumed to have equal volume in the simulations; this is a necessary hypothesis in order to obey the rules of the Flory–Huggins theory and DPD.³²

2.2. Mesoscale Simulation Method: Dissipative Particle Dynamics. Our overall strategy for investigating the order–order transition phenomenon consists of first exploring the microphase segregation process or ordered microphase formation via the order–disorder transition and then studying the microphase evolution process during thermal heating via the order–order transition. We simulate via the dissipative particle dynamics (DPD) method introduced by Hoogerbrugge and Koelman.^{33,34} For a thorough account on DPD, see refs 33–38. In this kind of simulation, a particle represents a small segment of a polymer chain and moves in free space under the three forces acting on it. These DPD particles are subject to soft potentials and governed by predefined collision rules. Like molecular dynamics (MD), the DPD particles obey Newton's equation of motion.

In the PS–PI diblock copolymer, there are two different species of DPD particles: poly(styrene) particles (PS) and poly(isoprene) particles (PI). Each particle was subject to soft

interactions with its neighbors via three forces: conservative (\mathbf{F}_{ij}^C), dissipative (\mathbf{F}_{ij}^D) and random forces (\mathbf{F}_{ij}^R). All the forces between particles i and j vanish beyond a cutoff radius r_c , which is usually chosen as the reduced unit of length, $r_c \equiv 1$. The conservative force for nonbonded particles is defined by soft repulsion

$$\mathbf{F}_{ij}^C = \begin{cases} a_{ij}(1 - r_{ij})\hat{\mathbf{r}}_{ij} & (r_{ij} \leq 1) \\ 0 & (r_{ij} > 1) \end{cases} \quad (1)$$

where a_{ij} is the maximum repulsion strength between particles i and j and $\mathbf{r}_{ij} = \mathbf{r}_i - \mathbf{r}_j$, $r_{ij} = |\mathbf{r}_{ij}|$, $\hat{\mathbf{r}}_{ij} = \mathbf{r}_{ij}/r_{ij}$. The parameter a_{ij} , henceforth referred to as the bead–bead repulsion parameter or simply as the DPD interaction parameter, depends on the underlying atomistic interactions and is related to the parameter χ of section 2.1. The relationship between a_{ij} and χ has been established by Groot and Warren³⁶ as

$$a_{ij} = a_{ii} + 3.497\chi_{ij} \quad \text{for } \rho = 3 \quad (2)$$

where $a_{ij} = 25$ leads to the compressibility of water. Note that using this equation implies that if the species are compatible, $\chi_{ij} \approx 0$ and $a_{ij} = 25$.

For bonded bead on the copolymers, the interaction force is:

$$\mathbf{F}_{ij}^C = \left[-\sum_j C r_{ij} \hat{\mathbf{r}}_{ij} \right] \quad (3)$$

where the sum runs over all particles to which particle i is connected.

The dissipative and random forces are given by

$$\mathbf{F}_{ij}^D = [-\gamma \omega^D(r_{ij})(\mathbf{v}_{ij} \cdot \hat{\mathbf{r}}_{ij}) \hat{\mathbf{r}}_{ij}] \quad (4)$$

$$\mathbf{F}_{ij}^R = (\sigma \omega^R(r_{ij}) \xi_{ij} \hat{\mathbf{r}}_{ij}) \quad (5)$$

where γ is the dissipation strength, σ is the noise strength, ω^D and ω^R are r -dependent weight functions, $\mathbf{v}_{ij} = \mathbf{v}_i - \mathbf{v}_j$, and ξ_{ij} is a Gaussian noise term with the following properties: $\xi_{ij} = \xi_{ji}$, $\langle \xi_{ij}(t) \rangle = 0$, $\langle \xi_{ij}(t) \xi_{kl}(t') \rangle = (\delta_{ik} \delta_{jl} + \delta_{il} \delta_{jk}) \delta(t - t')$. The choice of the weight functions is not specified by the method, but Español and Warren³⁵ showed that they should be related in accordance with

$$\omega^D(r) = [\omega^R(r)]^2 \quad (6)$$

in order for the DPD system to have a well-defined equilibrium state obeying Boltzmann statistics. If the previous equation is satisfied, the equilibrium temperature is defined as $k_B T = \sigma^2 / (2\gamma)$. This condition fixes the temperature of the system and relates it to the two DPD parameters γ and σ ($k_B T$ is usually chosen as the reduced unity of energy). For simplicity, the weight functions are usually chosen to be similar to the form of the conservative force, so

$$\omega^D(r) = [\omega^R(r)]^2 = \begin{cases} (1 - r)^2 & (r \leq 1) \\ 0 & (r > 1) \end{cases} \quad (7)$$

All the forces are pairwise additive, central, and satisfy Newton's Third Law, thus conserving linear and angular momentum. In the mesoscopic simulation of the PS–PI copolymer, the dynamic behavior of the system is followed by integration of the equations of motion using a modified version of the Verlet algorithm.³⁹ Integration of the equations of motion for the PS–PI copolymer generates a trajectory through the system's phase from which thermodynamic observables may be constructed from a suitable average. From this information, the microphase separation process, ordered structures generation, order–disorder and order–order phase transition can be observed.

Table 1 shows the parameters used in the following simulations. Using eq 2 implies that if the species are compatible, $\chi_{ij} \approx 0$, and therefore $a_{ij} = 25$. The interaction parameters were accordingly chosen as $a_{S-S} = 25$ and $a_{I-I} = 25$, $a_{S-I} = 38$, the last value being deduced from eq 2 with $\chi_{ij} = 3.955$ (the value at $T = 300$ K, which is representative of the interaction PS–PI²⁴). The parameters were

Table 1. Parameter Values Used in the DPD Simulations for $k_B T = 1^a$

parameters	value
box size	$12 \times 12 \times 12$
cut-off radius r_c	1
noise strength σ	3
time step	0.05
dissipation strength γ	4.5
density ρ	3
repulsion strength a	25

^a All values are in DPD units.

used for the scan at $k_B T = 1$. For simulations where $k_B T \neq 1$, we still use eq 2, but we have verified that there is no qualitative change if $0.1 < \chi < 0.4$ (the values we have obtained in our simulations of ref 24, valid for $300 < T < 400$ K).

Because the equilibrium temperature is defined as $k_B T = \sigma^2/2\gamma$, changing $k_B T$ implies changing the value $\sigma^2/2\gamma$.

All simulations were carried out in a cubic box of $(12r_c, 12r_c, 12r_c)$ size, containing a total of 260 Gaussian chains, a spring constant $C = 4$, and a density $\rho = 3$. DPD simulations for the first part of this study were made at temperature $k_B T = 1$. In the second part, the temperature interval employed was from 1 to 2 in $k_B T$ reduced units. This allows for a reasonable and efficient relaxation for the poly(styrene)–poly(isoprene) diblock system.

A total of 10^5 time steps with step size of $\Delta t = 0.05$ in DPD reduced units are performed for equilibration. Each simulation on a PC with a CPU Pentium IV takes about 10 h of CPU time with a box size of 12^3 . If the box size is increased to 20^3 , the time for one simulation takes up to 2 days of CPU time.

3. Results and Discussion

3.1. Order–Disorder Phase Transition of PS–PI Copolymer. In this part, we show the formation of different ordered structures as the composition of PS–PI copolymer varies. The ordered structures generated in this way will be the basis for the temperature variation analysis of the order–order transition to be analyzed next.

In our simulation, all PS–PI diblock systems start from a random disordered state, where the polymers are in a homogeneous melted phase. We scanned the composition interval from 0.1–0.9 (volume fraction) of poly(styrene) with increments of 0.05. During the temperature relaxation (the system attains an equilibrium temperature $k_B T = 1$, DPD reduced units), we observed the microphase segregation and the generation of ordered structures. The transition from a homogeneous disordered phase of chains to a heterogeneous melt of ordered microphase-separated domains (first order transition) is defined to be an order–disorder transition (ODT) for the PS–PI system. As mentioned before, all simulations were carried out in a cubic box of $(12r_c, 12r_c, 12r_c)$ size, containing a total of 260 Gaussian chains. This size could seem small for present computer capabilities, but because the analyzed composition intervals are from 0.1 to 0.9 (volume fraction) of PS with increments of 0.05, it takes much more CPU time to scan the whole interval. To verify that the morphologies are not influenced by the size of the box or boundary conditions, selected calculations with a box of $(20r_c, 20r_c, 20r_c)$ size containing a total of 2400 Gaussian chains were performed. Our conclusion is that the morphologies are stable under an increasing system size. If the box size is increased to 20^3 , the time for one simulation takes up to 2 days of CPU time.

As shown in Figure 3 and Table 2, the simulation of the PS–PI diblock copolymer displays a rich variety of characteristic, stable ordered microphases in the composition interval analyzed. These include the following: (a) alternating lamellar (LAM), (b) ordered bicontinuous double diamond (OBDD), (c) hexagonal packed cylinders (HPC), and (d) body-centered-cubic (BCC). These results are in accordance with the mean-field

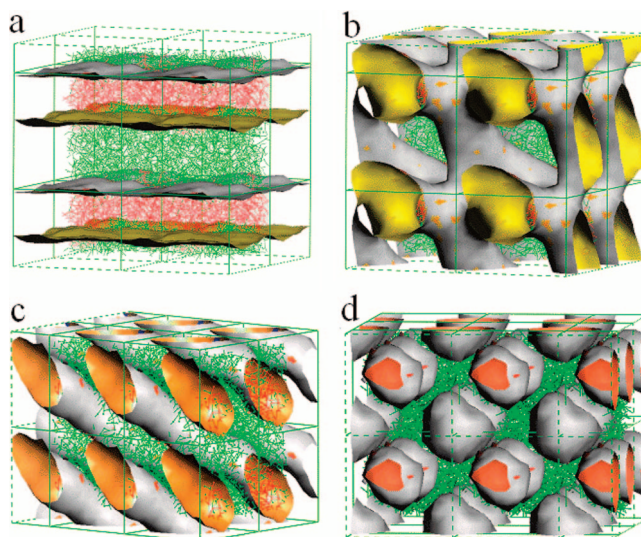


Figure 3. Representative ordered microphases of the $[PS]_n$ – $[PI]_m$ linear diblock copolymer obtained as the composition poly(styrene)/poly(isoprene) is changed (see Table 2). Key: (a) LAM (red or green are PS or PI microdomains); (b) OBDD (the gray regions are PI density surfaces); (c) HPC (orange regions are the caps of PS cylinders; gray regions are the PI cylinder density surfaces); (d) BCC (red regions and gray regions are PS and PI microdomains, respectively).

Table 2. Ordered Microphases Evolution with Equilibrium Structures of the $[PS]_n$ Diblock Copolymer

diblock copolymer $[PS]_n$ – $[PI]_m$ composition (volume fraction) PS/PI	microphase morphology (equilibrium structures)
0.1/0.90	body-centered cubic
0.15/0.85	body-centered-cubic
0.2/0.80	hexagonal packed cylinders
0.25/0.75	hexagonal packed cylinders
0.30/0.70	ordered bicontinuous double
0.35/0.65	lamellar
0.40/0.60	lamellar
0.45/0.55	lamellar
0.50/0.50	lamellar

theory of Leibler.³ In fact, his phase diagram for diblock copolymers in the weak segregation limit only predicts microphase separation from disorder to BCC, then to hex and then to the lamellar phase as the composition is varied. Our results agree with the experimentally determined phase diagram for PS–PI diblock copolymer by Khandpur et al.⁴⁰ These ordered microphase structures obtained via mesoscopic simulation for the PS–PI system can be compared positively with the transmission electron microscopic images reported by Aggarwal and Khandpur et al.^{40,41} In ref 24 and Figure 3, this has been analyzed in detail.

The tendency of PS–PI diblock copolymers to self-assemble into periodic structures depends upon molecular weight, styrene–isoprene interaction, and, most importantly, composition. The shape of the poly(styrene)/poly(isoprene) interface varies with the relative chain length of the component homopolymers. A symmetric PS–PI diblock copolymer (i.e., when volume fractions of both blocks are equivalent) forms an ordered microphase with lamellar interfaces (LAM) formed from alternating poly(styrene) and poly(isoprene) microdomains, as shown in Figure 3a. When the volume fraction of a component (PS block) increases in relation to other component (PI block), the interface tends to become curved. This is because the chains of a component are more extended, allowing the formation of less planar interfaces. In this case, the conformational entropy lost from the majority component is too high. Therefore, to gain conformational entropy, the chains of the majority component tend to expand along the direction parallel to the interface.

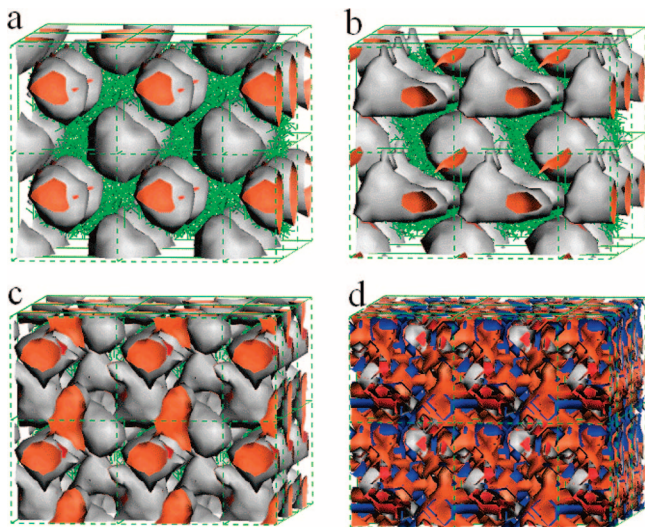


Figure 4. Thermally induced phase transition from body-centered-cubic to homogeneous phase at a temperature $k_B T = 1.8$: (a) initial BCC system, $t = 0$; (b) and (c) intermediate images showing the deformation of BCC state to irregular spheres; (d) melt system of poly(styrene) and poly(isoprene) chains showing the formation of the homogeneous phase at the equilibration temperature.

Consequently, the PS/PI interface becomes convex toward the minority component. The interface curvature effect is more pronounced when the composition between PS and PI blocks of the PS–PI copolymer is more asymmetric. Therefore, an OBDD structure at the composition of 0.3/0.7 (volume fraction) was observed (see Figure 3b). The HPC structure was obtained at the composition interval between 0.25/0.8 and 0.25/0.75, (Figure 3c) and the BCC microphase was observed at the composition interval between 0.1/0.9 and 0.15/0.85 (Figure 3d). In all cases, the microphases obtained showed rich microdomains of a single type of homopolymer poly(styrene)/poly(isoprene) separated by interfaces. These packings were more pronounced in the HPC and BCC structures.

3.2. Order–Order Phase Transition of BCC, HPC, OBBD, and LAM Structures. The ordered microphases in the PS–PI copolymer are altered through temperature variations. In other words, the periodic morphology changes of diblock copolymers are accessible by thermotropic order–order transitions. A huge number of previous experimental investigations have reported phase transitions of block copolymers between cylinders and spheres.^{11,21,42–44} Most of these phase transitions have been induced via temperature controls near the phase boundary at a given volume fraction of each block. Recently, several reports have proposed that the phase transition between cylinders to spheres via temperature effects occurs by way of a breaking-down process.^{17,20} With this in mind, to simulate the thermotropic changes of the ordered microphases of the PS–PI system referred to before, ordered structures with compositions near the boundaries between different microphases were put through continuous cycles of thermal heating and cooling.

3.2.1. Body-Centered-Cubic Microphase: Thermal Study. The equilibrium ordered microphase with BCC arrangement at temperature $k_B T = 1$ (Figure 3d), was put through thermal heating cycles in the temperature interval $k_B T = 1$ to $k_B T = 2$ in DPD units with increments of 0.1. A total of 2.0×10^5 time steps with step sizes of $\Delta t = 0.05$ were allowed for temperature equilibration in each temperature increment. The transition from the ordered BCC phase to the melted phase was already observed for $k_B T = 1.8$. This is shown in Figure 4a–d. Figure 4a corresponds to the initial ordered state, $t = 0$, and as time

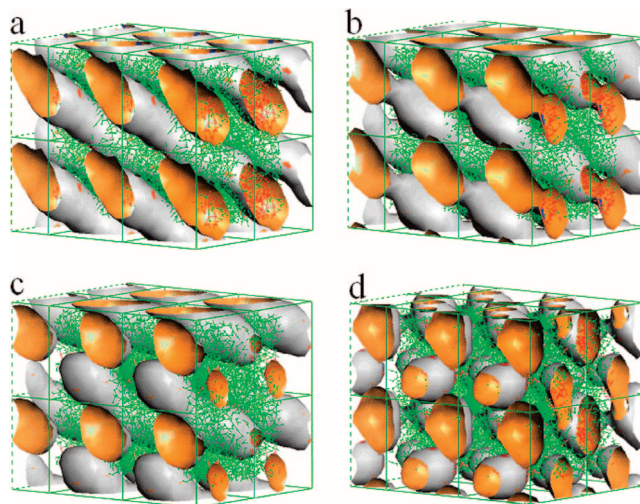


Figure 5. Thermally induced phase transition from the hexagonal-packed cylinders phase to a body-centered cubic state, on a PS–PI asymmetric copolymer at temperature $k_B T = 1.5$: (a) HPC microphase; (b) undulation process of poly(styrene) microdomains in the poly(isoprene) matrix by anisotropic composition fluctuations due to heating; (c) breakdown of PS undulated microdomains and metastable microdomains formation of outstretched spheres; (d) stabilization and evolution of outstretched spheres to BCC states.

goes on, the spheres begin to deform (Figure 4b,c) until the disordered state is attained (Figure 4d) at equilibrium. For higher temperatures, the effect is the same; the spherical microphase evolves into a homogeneous disordered state (melt copolymer). This observation is in accordance with the phase diagram of temperature vs composition reported by Sakurai et al.⁸ (which is the temperature vs composition version of Leibler's diagram (Figure 1)).

At the new equilibrium temperature ($k_B T = 1.8$), a dense collection of monodisperse copolymer chains (styrene–isoprene) will be arranged in minimum free energy configurations in the melt phase. In the heating process of BCC microphases, two thermodynamics effects (enthalpy and entropy) govern the microphase behavior. The enthalpy is proportional to the Flory–Huggins segmental interaction parameter, which is found to be inversely proportional to temperature. During the temperature increase, the segment–segment interaction parameter between styrene and isoprene decreases, and therefore it disfavors an increase in styrene–isoprene contacts, generating the deformation from spherical arrangements into irregular spheres (Figure 4b,c) until reaching a melted state (Figure 4d). The enthalpic factor in the thermal heating process is accompanied by an increase in entropy. Entropy is a measure of the system randomness brought about by thermal motion of diblock chains. At higher temperatures, the entropy dominates (the chains configuration becomes less constrained) and the block chains of PS–PI copolymer mix randomly to form a homogeneous (disordered) material.

The inverse process from the homogeneous melt phase ($k_B T = 1.8$ to $k_B T = 1$) was performed. The spherical ordered BCC microphase was obtained after the temperature equilibration and thermoreversibility was confirmed. The thermoreversible transition process is driven by thermodynamic instability. When the temperature is reduced, the general tendency of styrene–isoprene blocks is to segregate; i.e., the enthalpic process of demixing is favored. The segregation process between styrene and isoprene chains generate the styrene microdomains nucleation process (spherical microdomains) in the matrix of the majority component (isoprene). During the thermoreversible process, we

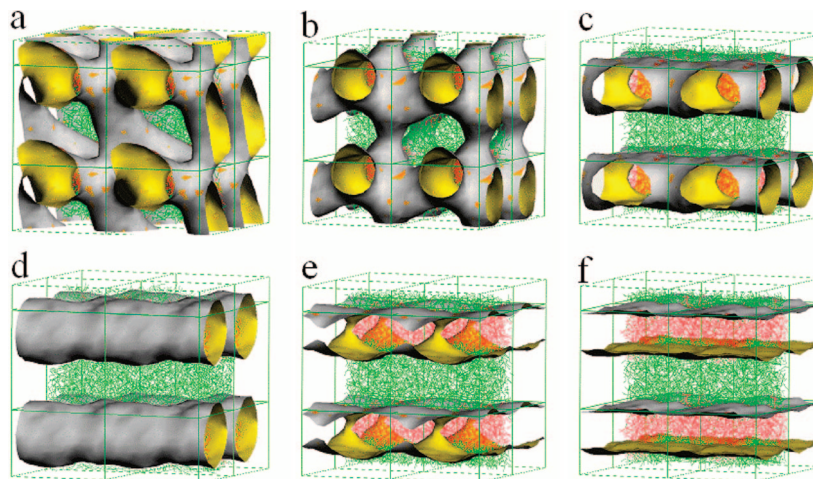


Figure 6. Order–order phase transition from an ordered bicontinuous double diamond to the lamellar microphase, on a PS–PI asymmetric copolymer at temperature $k_B T = 2$. Key: (a) initial OBDD microphase before the thermal heating process; (b) interconnection fluctuations of the OBDD microphase by anisotropic composition fluctuations due to heating; (c) formation of the first metastable estate, HPL; (d) metastable structure fluctuations between HPL and cylinder microphases (second metastable estate); (e, f) thermally induced phase transition from the HPL metastable state to the LAM microphase.

could not find formation of metastable structures in the BCC system in the vicinity between spherical and cylinders.

3.2.2. Hexagonal Packed Cylinders Microphase: Thermal Study. In the melts, block copolymers can undergo a type of microphase modification to produce coexisting intermediate phases that are spatially periodic. It is known that PS–PI diblock copolymers can develop long-lived transient or metastable structures during an order–order phase transition because of energetic barriers and sluggish molecular motion. These metastable structures or intermediate states can be detected and controlled by a continuous temperature increase during the simulation. In Figure 5a–d, the results of a thermally induced phase transition from the HPC microphase to BCC are shown. The results show that the transformation from the HPC to BCC microphases via temperature effects proceeds in several stages. Initially, the HPC microdomains display undulation of the PS/PI interphase induced by thermodynamic instability (entropic effects) (Figure 5a,b). The configuration of poly(styrene) chains (governed by entropic interactions) in the cylindrical microdomains and in the PS/PI interphase becomes less rigid due to temperature effects, and the poly(styrene) chain movements modify the poly(styrene) microdomain shapes via composition fluctuation effects. These are known as thermally induced anisotropic composition fluctuations.²⁰ With the temperature increase, the anisotropic composition fluctuations reach an instability critical point. The undulating cylindrical microdomains break down and induce the formation of ellipsoids (Figure 5c). At the equilibration temperature $k_B T = 1.5$, the ellipsoid's transitional state evolves into BCC structures. In this thermally induced stage, the uniform spherical microdomains are stabilized (Figure 5d). This behavior is in agreement with the reported experimental observation by Kimishima and Hashimoto.²¹ In this experimental study, they establish the mechanism of undulation and breakdown for order–order transitions in a block copolymer. The behavior of the order–order transition between cylindrical to spherical structures found in our simulations is in agreement with Figure 1. An equilibrium structure change for the specific case of a HPC microphase transitioning to a BCC system by temperature effects via order–order phase transition can be generated.

The thermoreversible transition process from the BCC state to HPC arrangement ($k_B T = 1.5$ to 1) in the PS–PI diblock copolymer was performed. The reverse microphase transition of the PS–PI system involves deformation and elongation

of spheres into ellipsoids and coalescence of ellipsoids into a cylinder. These processes are driven by thermodynamic instability of the spherical interface caused by increased segregation.²¹

3.2.3. Ordered Bicontinuous Double Diamond Microphase: Thermal Study. Although the ordering kinetics of order–order transitions have been well investigated for the HPC microphase,^{20,21} the dynamic transformation of other ordered structures such as OBDD and LAM have been less explored. The OBDD microphase of the PS–PI diblock copolymer (Figure 6a) was subject to thermal heating cycles from $k_B T = 1$ to $k_B T = 2$. In Figure 6a–f, the results of the thermally induced microphase transition of the OBDD system are shown. The transformation from the gyroid to lamellar structures by temperature effects proceeds via the generation of two coexisting intermediate microphases (metastable states). Initially the OBDD microdomains display an undulation process. In this case, the thermodynamic instability induces an anisotropic composition fluctuation of poly(styrene) microdomains interconnections and a decrease of volume in the side interconnections is observed (Figure 6a,b). As time goes on, the anisotropic composition fluctuations induce the breakdown of side interconnections in the gyroid structure, generating metastable microphases with hexagonal perforated layers (HPL) (Figure 6c). This evolves into an equilibrium energetic region where the thermotropic interactions are constant and the poly(styrene) microdomain motion is slow. This explains why the HPL microphases are more stable than other metastable structures (Figure 6b,c). When the system is subject to a higher temperature, $k_B T = 2$, the HPL microphase is unstable. The cylindrical metastable microphase evolves by interfacial instability between poly(styrene) and poly(isoprene) microdomains (Figure 6d). The cylindrical structure is unstable due to the anisotropic composition fluctuation increment from temperature effects. This metastable state displays a fluctuation process between HPL and cylinder microphases (Figure 6d,e). At the equilibration temperature $k_B T = 2$, the poly(styrene) cylinder microdomains are joined together to evolve into undulating lamellar microphases. In this thermal stage, the uniform LAM microphases are stabilized (Figure 6f). The phase diagram of temperature vs composition reported by Sakurai et al.⁸ (Figure 1) does not consider the OBDD microphase, and therefore, it does not completely describe the behavior of the order–order transition process in the vicinity between the OBDD and LAM microphases.

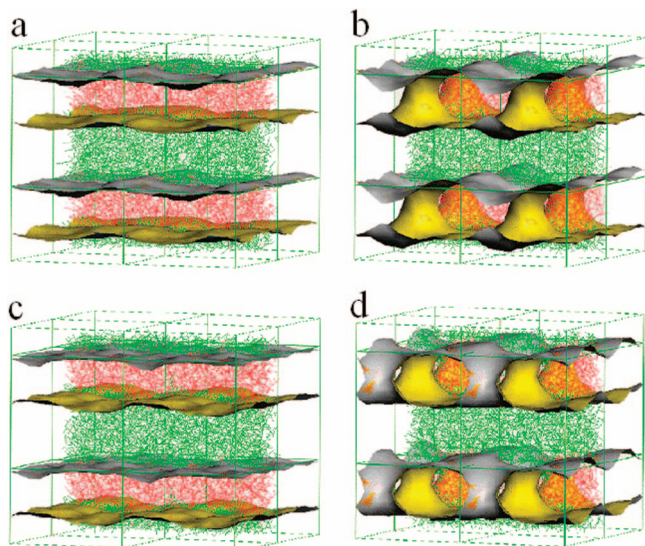


Figure 7. Order–order transition from the lamellar phase to the hexagonal perforated layer, on a PS–PI asymmetric copolymer at temperature $k_B T = 2$. Key: (a) Initial lamellar structure of PS and PI microdomains before the heating process; (b and c) fluctuation of lamellar phase to hexagonal perforated layer observed during heating process and system stabilization; (d) stable perforated layer.

The reversible transition process from the lamellar state to the gyroid arrangement ($k_B T = 2$ to $k_B T = 1$) was monitored. The reverse microphase transition involves deformation of the lamellar microphase (interface undulation effect), formation of metastable structures (cylinders and hexagonal perforated layers) and coalescence of the hexagonal perforated layers into the gyroid structure. The transition is thus thermoreversible.

3.2.4. Lamellar Microphase: Thermal Study. According to the diagram in Figure 1, the transition from LAM to other structures upon raising the temperature proceeds via cylinders (HPC) and spheres (BCC), except at $f = 0.5$ (critical point, order–disorder transition). This phase diagram does not consider the metastable microphase of hexagonal perforated layers, and therefore it is not adapted to describe the behavior of order–order transition process in the vicinity between lamellar and hexagonal perforated layers microphases. However, evidence of a thermally reversible order–order transition between lamellar and perforated layers microphases was reported by Mani et al.⁴⁵ Our simulations are able to describe this transition. In Figure 7a–d, we show the results of the thermally induced order–order transition from the LAM to the HPL microphase (in the vicinity between the lamellar and the gyroid microphase, Table 2), deduced from a PS–PI asymmetric copolymer (0.35/0.65, composition) at a temperature $k_B T = 2$. Results of the mesoscale simulation show that the transformation from the lamellar structure to the hexagonal perforated layer microphases by temperature effects proceeds via a long-lived transient process. The transformation from the lamellar structure to the HPL microphases by temperature effects proceeds via anisotropic composition fluctuations in the PS/PI interface. The thermodynamic instability of poly(styrene) linear microdomains induce interconnections between poly(isoprene) alternate layers (Figure 7a,b), and these fluctuations cause alternations between the two structures (Figure 7b,c). At the equilibration temperature, $k_B T = 2$, the HPL metastable state reaches high stability (Figure 7d), and perforated lamellar microphases of alternating PS and PI lamellae with hexagonal-packed PI connectors perforating the PS phase are obtained.

The reversible process from the HPL state to the lamellar arrangement ($k_B T = 2$ to $k_B T = 1$) was also performed. The reverse microphase transition involves the instability of the

poly(isoprene) microdomains interconnections, PS and PI microdomain segregation and coalescence of the HPL state to the lamellar microphase. The process is thus thermoreversible.

4. Conclusions

We have performed mesoscale simulations to explore the different phase transitions of characteristic structures of poly(styrene)–poly(isoprene) diblock copolymer in the bulk state. By varying the compositions of the poly(styrene)–poly(isoprene) diblock system, a display of rich variety of characteristic ordered microphases are observed: body-centered-cubic (BCC), hexagonal packed cylinders (HPC), alternating lamellar (LAM), and ordered bicontinuous double diamond (OBDD).

The BCC, HPC, OBDD, and LAM microphases were subjected to thermal cycles of heating and cooling over an interval of reduced temperature. The thermodynamic instability of poly(styrene)–poly(isoprene) microdomains, due to enthalpic and entropic interactions by the temperature effect induce anisotropic composition fluctuations (microphase instability) and hence modify the PS/PI interphase, generating microphase transformations via order–order process. To show the effect of temperature, we started from a “quenched” morphology at $k_B T = 1$ and then the specimens were subject to thermal annealing at $k_B T \neq 1$.

The BCC structure microphases disappear on increasing the temperature (continuous heating cycles). This microphase did not present an order–order structure transformation, but only generates a homogeneous phase (melted phase). In the case of the HPC microphase, we observed the order–order transition process from HPC to BCC during the thermal heating process. The process take place in several stages: microdomains undulation process, microphase modification, breakdown of undulated microdomains and thermal stabilization of poly(styrene) microdomains in the new ordered state. This agrees well with the phase diagram of Leibler’s weak segregation limit theory.

The transformation from the OBDD to lamellar structures proceeds via the generation of two coexisting intermediate metastable microphases: hexagonal perforated layers and cylinders. Finally, we found a transition between lamellar and hexagonal perforated layer microphases.

By performing a cooling process it was shown that the order–order transition processes between all different kinds of ordered microphases of PS–PI diblock copolymer are thermoreversible. The value of our simulations resides, within the limitations of a DPD simulation, in that it allows one to visualize the evolution from one order state to other as temperature is raised. One of the limitations is that there is no a direct connection between reduced units and experimental values.

Acknowledgment. The authors acknowledges the Instituto Mexicano del Petróleo (IMP) for technical support of this work. We also thank the Universidad Nacional Autónoma de México (UNAM) and PAPITT Project No. IN101008.

References and Notes

- (1) Bates, F. S. *Annu. Rev. Phys. Chem.* **1990**, *41*, 525–557.
- (2) Hamley, I. W. *The Physics of Block Copolymers*; Oxford University Press: Oxford, U.K., 1998.
- (3) Leibler, L. *Macromolecules* **1980**, *13*, 1602–1607.
- (4) Matsen, M. W.; Bates, F. S. *Macromolecules* **1996**, *29*, 1091–1098.
- (5) Fredrickson, G. H.; Helfand, E. J. *Chem. Phys.* **1987**, *87*, 697–705.
- (6) Brazovskii, S. A. *Sov. Phys. JETP* **1975**, *41*, 85.
- (7) Almdal, K.; Koppi, K. A.; Bates, F. S.; Mortensen, K. *Macromolecules* **1992**, *25*, 1743–1751.
- (8) Sakurai, S.; Kawada, H.; Hashimoto, T.; Fetters, L. J. *Macromolecules* **1993**, *26*, 5796–5802.
- (9) Han, C. D.; Baek, D. M.; Kim, J. K. *Macromolecules* **1990**, *23*, 561–570.

- (10) Han, C. D.; Baeck, D. M.; Kim, J. K.; Ogawa, T.; Hashimoto, T. *Macromolecules* **1995**, *28*, 5043–5062.
- (11) Krishnamoorti, R.; Modi, M. A.; Tse, M. F.; Wang, H.-C. *Macromolecules* **2000**, *33*, 3810–3817.
- (12) Kim, E. Y.; Lee, D. J.; Kim, J. K. *Macromolecules* **2006**, *39*, 8747–8757.
- (13) Sakamoto, N.; Hashimoto, T.; Han, C. D.; Kim, D.; Vaidya, N. Y. *Macromolecules* **1997**, *30*, 1621–1632.
- (14) Court, F.; Yamaguchi, D.; Hashimoto, T. *Macromolecules* **2006**, *39*, 2596–2605.
- (15) Bodycomb, J.; Yamaguchi, D.; Hashimoto, T. *Macromolecules* **2000**, *33*, 5187–5197.
- (16) Modi, M. A.; Krishnamoorti, R.; Tse, M. F.; Wang, H.-C. *Macromolecules* **1999**, *32*, 4088–4097.
- (17) Sakurai, S.; Kawada, H.; Hashimoto, T.; Fetters, L. W. *Macromolecules* **1993**, *26*, 5796–5802.
- (18) Modi, M. A.; Krishnamoorti, R.; Tse, M. F.; Wang, H.-C. *Macromolecules* **1999**, *32*, 4088–4097.
- (19) Kim, J. K.; Lee, H. H.; Gu, Q.-J.; Chang, T.; Jeong, Y. H. *Macromolecules* **1998**, *31*, 4045–4048.
- (20) Ryu, C. Y.; Lodge, T. P. *Macromolecules* **1999**, *32*, 7190–7201.
- (21) Kimishima, K.; Koga, T.; Hashimoto, T. *Macromolecules* **2000**, *33*, 968–977.
- (22) Soto-Figueroa, C.; Rodríguez-Hidalgo, M. R.; Martínez-Magadán, J. M. *Polymer* **2005**, *46*, 7485–7493.
- (23) Soto-Figueroa, C.; Luis-Vicente, J. M.; Martínez-Magadán, J. M.; Rodríguez-Hidalgo, M. R. *Polymer* **2007**, *48*, 3906–3911.
- (24) Soto-Figueroa, C.; Luis-Vicente, J. M.; Martínez-Magadán, J. M.; Rodríguez-Hidalgo, M. R. *J. Phys. Chem. B* **2007**, *111*, 11756–11764.
- (25) Accelrys, Material studio release, notes, release 4.2; Accelrys Software, Inc.: San Diego, CA, 2006.
- (26) Doi, M.; Edwards, S. F. *The Theory of Polymer Dynamics*. Oxford University Press: **1998**.
- (27) Flory, P. J. *J. Chem. Phys.* **1941**, *9*, 660–671.
- (28) Huggins, M. L. *J. Chem. Phys.* **1941**, *9*, 440.
- (29) Fan, F. C.; Olafson, B. D.; Blanco, M.; Hsu, S. L. *Macromolecules* **1992**, *25*, 3667–3676.
- (30) Mark, J. E. *Polymer data handbook*; Oxford University Press: Oxford, U.K., 1999.
- (31) Bicerano, J. *Prediction of Polymer Properties*, 3rd ed.; Marcel Dekker: Midland, MI, 2002.
- (32) Maiti, A.; McGrother, S. J. *J. Chem. Phys.* **2004**, *120*, 1594–1601.
- (33) Hoogerbrugge, P. J.; Koelman, J. M. V. A. *Europhys. Lett.* **1992**, *19*, 155–160.
- (34) Koelman, J. M. V. A.; Hoogerbrugge, P. J. *Europhys. Lett.* **1993**, *21*, 363–368.
- (35) Español, P.; Warren, P. B. *Europhys. Lett.* **1995**, *30*, 191.
- (36) Groot, R. D.; Warren, P. B. *J. Chem. Phys.* **1997**, *107*, 4423–4435.
- (37) Groot, R. D.; Madden, T. J. *J. Chem. Phys.* **1998**, *108*, 8713–8724.
- (38) Groot, R. D.; Madden, T. J.; Tildesley, D. J. *J. Chem. Phys.* **1999**, *110*, 9739–9749.
- (39) Verlet, L. *Phys. Rev.* **1967**, *159*, 98–103.
- (40) Khandpur, A. K.; Forster, S.; Bates, F. S. *Macromolecules* **1995**, *28*, 8796–8806.
- (41) Aggarwal, S. L. *Polymer* **1976**, *17*, 938–956.
- (42) Krishnamoorti, R.; Silva, A. S.; Modi, M. A.; Hammouda, B. *Macromolecules* **2000**, *33*, 3803–3809.
- (43) Sota, N.; Hashimoto, T. *Polymer* **2005**, *46*, 10392–10404.
- (44) Sakamoto, N.; Hashimoto, T. *Macromolecules* **1998**, *31*, 8493–8505.
- (45) Mani, S.; Weiss, R. A.; Cantino, M. E.; Khairallah, L. H.; Hans, S. F.; Williams, C. E. *Eur. Polym. J.* **2000**, *36*, 215–219.

MA7028264